Thermochimica Acta 480 (2008) 30–34

Contents lists available at ScienceDirect

Thermochimica Acta

journal homepage: www.elsevier.com/locate/tca

Thermal analysis of bis(tetraethylammonium) tetrachloroferrate(II)

Emilia Styczeń[a], Agnieszka Pattek-Janczyk[b], Maria Gazda[c], Wojciech K. Jóźwiak[d], Dariusz Wyrzykowski[a], Zygmunt Warnke[a,*]

[a] Faculty of Chemistry, University of Gdańsk, Sobieskiego 18, 80-952 Gdańsk, Poland
[b] Faculty of Chemistry, Jagiellonian University, Ingardena 3, 30-060 Kraków, Poland
[c] Faculty of Physics and Mathematics, Technical University of Gdańsk, Narutowicza 11/12, 80-952 Gdańsk, Poland
[d] Institute of General and Ecological Chemistry, Technical University of Łódź, Żwirki 36, 90-924 Łódź, Poland

ARTICLE INFO

Article history:
Received 19 August 2008
Received in revised form
18 September 2008
Accepted 24 September 2008
Available online 8 October 2008

Keywords:
Tetrahalogenoferrates(II)
Thermal decomposition
Mössbauer spectroscopy

ABSTRACT

Thermal decomposition of bis(tetraethylammonium) tetrachloroferrate(II) has been studied using the TG-FTIR, TG–MS and DTA techniques. The measurements were carried out in an inert atmosphere over the temperature range of 293–1073 K. The solid products of the thermal decomposition were identified by the FT-FIR, Mössbauer spectroscopy as well as the X-ray powder diffractometry. The influence of the oxidation state and the nature of a metal on thermal transformation profiles of analogous complexes have been discussed.

1. Introduction

The ferric(II) ion has been found to form with halide ligands high-spin tetrahedral complex ions, $[FeX_4]^{2-}$ [1,2]. Up to now, mostly structural [2] and spectroscopic [3–7] features of the halogen complexes of the ion have been studied. In addition, their magnetic properties aroused some interest, in particular owing to the large magnetic moment of $(Et_4N)_2[FeCl_4]$ (5.39 B.M.) [3,8]. Similar to analogous tetrachloroferrates(III), $[FeCl_4]^-$, their use as components of molecular magnetic conductors [9,10] has extensively been surveyed. Bearing in mind that use, it is highly probable that useful information on the properties of those materials might be obtained from the results of investigation of their thermal behaviour.

Our previous studies were concerned with the properties of analogous tetrahalogenoferrates(III) [11–17], in particular the thermal ones. Hence, the purpose of this contribution was the preparation of the $(Et_4N)_2[FeCl_4]$ complex and investigation of its thermal behaviour to bridge up the literature gap. Furthermore, it seemed worthwhile to compare the characteristic features of the ferric(II) compounds with those of the previously studied ferric(III) complexes, a particular emphasis being laid on their thermal characteristics.

2. Experimental

2.1. Synthesis of $(Et_4N)_2[FeCl_4]$

Bis(tetraethylammonium) tetrachloroferrate(II) was obtained using a procedure similar to that reported in the literature [3]. Thus, $FeCl_2$ (0.03 mol) was dissolved in a small volume of methanol and acetone, then the solution was added to a methanolic Et_4NCl (0.06 mol) solution, in an argon atmosphere. The solvents had previously been 'deoxygenated' by passing argon through them. The solid product was isolated rapidly by filtration under argon, dried in a stream of argon and finally placed in a closed container in a vacuum desiccator.

Elementary analysis confirmed the composition of the obtained compound (Found: C, 41.9; N, 6.0; H, 8.9. Calcd. for $[Et_4N]_2[FeCl_4]$, C, 41.9; N, 6.1; H, 8.7%) and FT-FIR [4] and Raman [5] spectroscopies additionally identified the complex.

2.2. Instrumental

The FTIR spectra were recorded on Bruker IFS 66 spectrophotometer in KBr pellets over the 4400–650 cm^{-1} range and the FT-FIR spectra (650–50 cm^{-1}) were taken in PE.

The TG-FTIR analyses were run in argon (Ar 5.0) on a Netzsch TG 209 apparatus coupled with Bruker FTIR IFS 66 spectrophotometer (range 298–1073 K, corundum crucible, sample mass *ca.* 12 mg, heating rate 15 K/min, flow rate of the carrier gas 18 mL/min).

* Corresponding author. Tel.: +48 58 3450360; fax: +48 58 3410357.
E-mail address: warnke@chem.univ.gda.pl (Z. Warnke).

0040-6031/$ – see front matter © 2008 Elsevier B.V. All rights reserved.
doi:10.1016/j.tca.2008.09.022

Table 1
Analyses of the decomposition products obtained in the inert atmosphere.

Complex	Stage	Temperature range (K)	DTG_{max} (K)	Mass loss (%)	Solid decomposition product
$(Et_4N)_2[FeCl_4]$	1	533–588	579	39	
	2	588–678	650	35	$FeCl_2$
	3	678–1023		13	$FeCl_2$, Fe_3C

The TG–DTA measurements were run in helium on a Setsys 16/18 thermoanalyzer (Setaram) coupled with a Thermostar quadrupole mass spectrometer (range 290–1123 K, corundum crucible, sample mass *ca.* 4–5 mg, heating rate 5 K/min, flow rate of the carrier gas 15 ml/min).

The course of thermal analysis was broken at points corresponding to the main steps of decomposition and the residues in the crucible were quickly cooled in the stream of argon. This enabled to analyze the residues at strictly pre-determined steps of decomposition. The analysis was carried out using the FTIR and Mössbauer spectroscopic techniques as well as the X-ray powder diffractometry.

The presence of crystalline phases was checked by X-ray diffraction with the use of Philips X'Pert diffractometer system. The XRPD patterns were recorded at room temperature with Cu Kα radiation (λ = 1.5418 Å). Qualitative analysis of the diffraction spectra was carried out with the ICDD PDF database [18].

The Mössbauer spectra were recorded at room temperature on a conventional spectrometer in transmission geometry using a ^{57}Co/Rh source. The samples were prepared in pellets with the thickness of *ca.* 10 mg Fe/cm^2. The spectra were numerically analyzed by the least-squares procedure assuming Lorentzian line shapes except for the original, non-burnt compound which was analyzed assuming the quadrupole splitting distribution. Isomer shifts are quoted relative to α-Fe.

3. Results and discussion

Results of the thermal analysis of $(Et_4N)_2[FeCl_4]$ are compiled in Table 1, whereas the shapes of the TG, DTG and DTA curves are presented in Fig. 1.

Bis(tetraethylammonium) tetrachloroferrate(II) undergoes thermal decomposition in the solid state, without melting, in three steps. The first step is fairly vigorous and immediately followed by the second one. Each of the steps is connected with a considerable mass loss, this making separation of the accompanying TG traces rather difficult. Fortunately, the sharp DTG and DTA peaks make possible to pinpoint the end of the first step and the onset of the other (588 K).

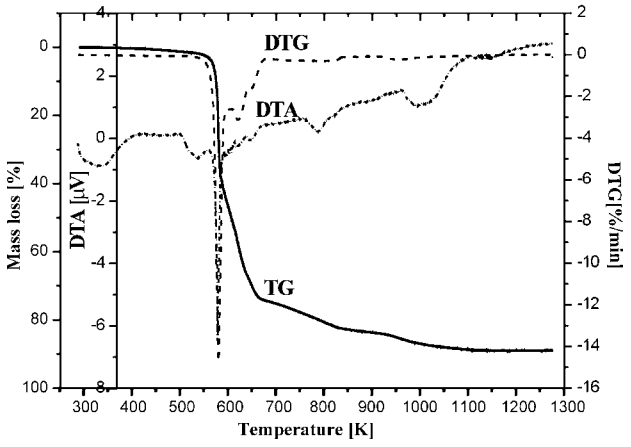

Fig. 1. TG, DTG and DTA curves of $(Et_4N)_2[FeCl_4]$ recorded in the inert atmosphere.

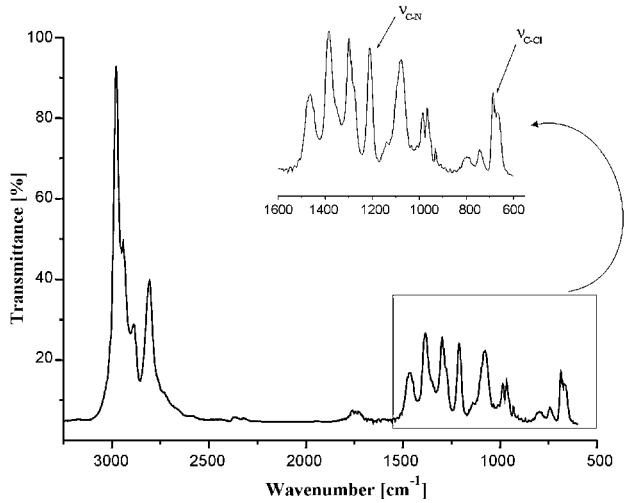

Fig. 2. FTIR spectrum of the volatile products of decomposition of $(Et_4N)_2[FeCl_4]$, in argon.

At the very beginning of the discussion, it is worthwhile to pay attention to a clear-cut difference between $(Et_4N)FeCl_4$ [17] and $(Et_4N)_2[FeCl_4]$. The former undergoes phase transformation (T_Φ = 427 K) followed by melting (T_m = 538 K) around the decomposition point (T_d = 563 K), while the latter retains its structure up to the decomposition point (T_d = 563 K). It neither undergoes phase transformation nor melts at all. In addition, the temperature of the first decomposition step of $(Et_4N)_2[FeCl_4]$ is by 30 K lower than that of $(Et_4N)[FeCl_4]$.

The volatile products of the $(Et_4N)_2[FeCl_4]$ were identified on the basis of their FTIR and TG–MS measurements (Figs. 2 and 3).

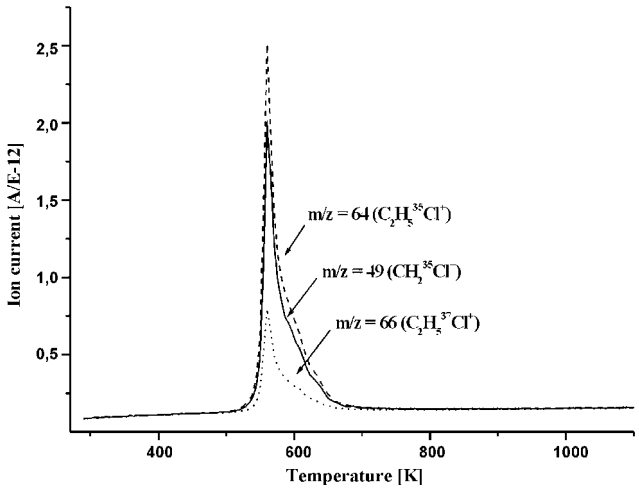

Fig. 3. Ionic current profiles recorded during TG–MS analysis of $(Et_4N)_2[FeCl_4]$ in the inert atmosphere.

The FTIR spectra of the compound cover the temperature range corresponding to the first two decomposition steps. Their shapes are alike thus indicating that at either step the same organic entity is released. Around 3000 cm^{-1}, bands due to C–H stretching vibrations of the methylene and methyl groups appear. The 1210 cm^{-1} band can be assigned to the stretching vibration of C–N, while the bands at 690 cm^{-1} are due to C–Cl. The latter band is missing in the original, non-burnt, compound indicating that during the first two steps the organic portion of the complex, i.e., the $(Et_4N)^+$ ion, undergoes degradation.

Having in hand decomposition patterns of similar compounds [17,19–21], it can be speculated that the volatile products are Et_3N and EtCl, as supported by inspection of the ion currents of the gaseous decomposition products. For instance, the peak at $m/z = 49$ can be assigned to $CH_2{}^{35}Cl^+$ resulting from fragmentation of the $C_2H_5{}^{35}Cl^+$ molecular ion ($m/z = 64$) and the peak $m/z = 66$ represents $C_2H_5{}^{37}Cl^+$ (Fig. 3). Respective curves as a function of temperature have identical shapes thus indicating EtCl as the product. In addition, taking into account calculations based on the mass losses taken from the TG curve, the first two decomposition steps can be described by the following equation:

$$(Et_4N)_2[FeCl_4] \underset{-2EtCl_{(g)},\, 2Et_3N_{(g)}}{\overset{533-678\,K}{\longrightarrow}} FeCl_2 + C_xH_yN_z \quad (1)$$

where $C_xH_yN_z$ denotes undecomposed organic residue

The loss in mass taken from the TG curve reveals the formation of $FeCl_2$ at 678 K. Sinters sampled at temperatures corresponding to the end of successive decomposition steps enabled identification of solid decomposition products. They were analyzed by spectroscopic techniques (FT-FIR, Mössbauer) and X-ray powder diffractometry of polycrystalline samples.

A comparison of the FT-FIR spectra (Fig. 4) allow to scan changes occurring in the immediate environment of the Fe^{2+} ion. Thus, in the FT-FIR spectrum of the non-burnt compound, bands due to metal–ligand vibrations are seen, namely $\delta_{Cl-Fe-Cl}$ (80 and 118 cm^{-1}) and ν_{Fe-Cl} (285 cm^{-1}) (Fig. 4(1)). The bands are also displayed in the spectrum of a sinter left behind after heating of $(Et_4N)_2[FeCl_4]$ up to 588 K (Fig. 4(2)). However, in this spectrum a new band at 316 cm^{-1} appears. This suggests only minor changes to have occurred within the co-ordination sphere of the central ion upon heating.

More pronounced changes occur during the second step of decomposition which product differs distinctly from that of the first step (Fig. 4(2 and 3)). The product is also retained in sinters sampled at higher temperatures (833 and 1073 K) as indicated by similarity of their FT-FIR spectra (Fig. 4(3–5)). Moreover, X-ray powder patterns of the sinters facilitate identification of the product (Fig. 5).

X-ray powder patterns of the sinters sampled at 673, 833 and 1073 K are almost identical thus indicating that the co-ordination sphere of iron(II) is thermally stable during the second decomposition step (673 K). The diffraction lines of the patterns correspond to X-ray reflections of $FeCl_2$. It suggests that the major product of the second and third steps of the thermal decomposition of $(Et_4N)_2[FeCl_4]$ is $FeCl_2$. To support this conclusion, especially in part concerning co-ordination sphere of the metal ion, Mössbauer spectra were recorded (Fig. 6). Their parameters are shown in Table 2.

The Mössbauer spectrum of the original, non-burnt $(Et_4N)_2[FeCl_4]$ reveals the internal doublet (Fig. 6(a)) which parameters were found assuming the quadrupole splitting distribution. The simple linear correlation between the isomer shift and the quadrupole splitting was also applied. The obtained average values of isomer shift IS = 0.92 mm/s with the sigma value of 0.06 mm/s and quadrupole splitting QS = 0.75 mm/s with the sigma

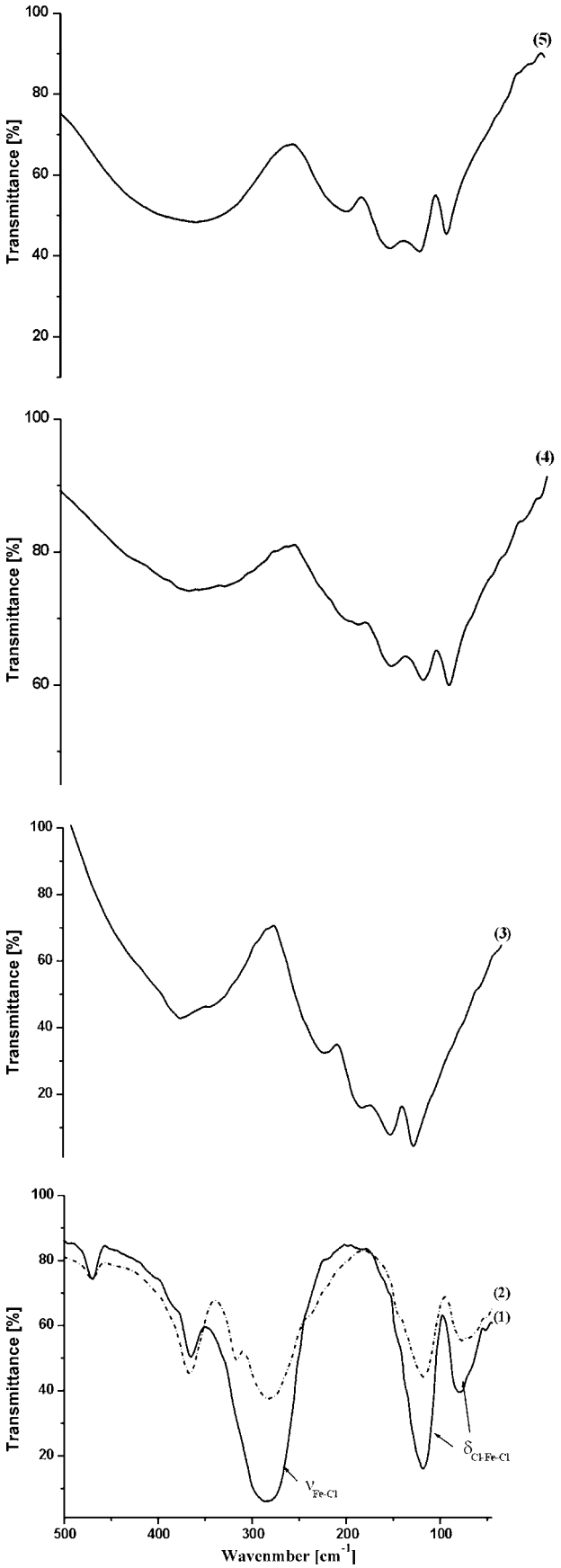

Fig. 4. The FT-FIR spectra of $(Et_4N)_2[FeCl_4]$ (1) and its decomposition products (2)–(5) at various temperatures: (2) $T_d = 588$ K; (3) $T_d = 673$ K; (4) $T_d = 833$ K; (5) $T_d = 1073$ K.

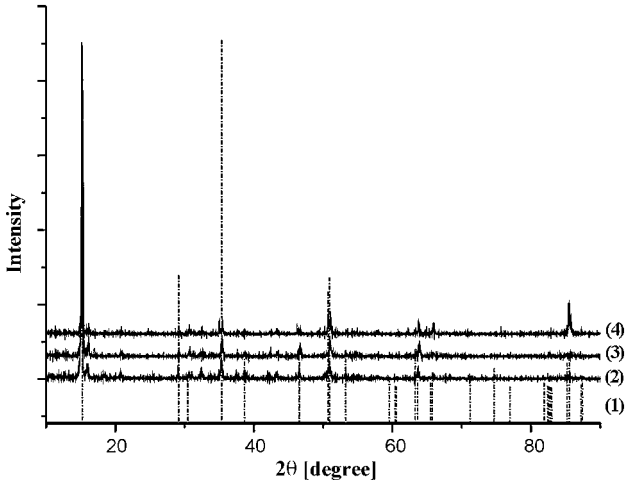

Fig. 5. XRPD pattern of $(Et_4N)_2[FeCl_4]$ heated up to 673 K (2), 833 K (3) and 1073 K (4) in argon. For comparison, reflections due to $FeCl_2$ (1) are shown.

value of 0.12 mm/s are compatible with the literature data for the tetrachloroferrate(II) ion [8,22].

After the second decomposition step (833 K) in the spectrum of the product two doublets – external (IS = 1.16(1) mm/s, QS = 2.32(1) mm/s) and internal (IS = 1.09(1) mm/s, QS = 0.76(1) mm/s) – appear (Fig. 6(b)). Their spectral parameters correspond to Fe(II) ions in different co-ordination environments. Internal doublet with parameters similar to the doublet in original sample may be attributed to the Fe^{2+} ions in the $[FeCl_4]^{2-}$ complex left after incomplete sample decomposition. On the other hand the external doublet dominating in the spectrum (87%) may be assigned to the Fe^{2+} ions probably existing in the $FeCl_2$ phase (as also supported by the XRPD and FT-FIR spectra).

It should also be noticed that when the sample was left in the apparatus overnight and the measurement was repeated, additional doublet with parameters of IS = 1.21(1) mm/s and QS = 2.99(1) mm/s has been found. These parameters correspond to those of $FeCl_2{\bullet}4H_2O$ [23]. This observation revealed hygroscopicity of the sample and confirmed the presence of $FeCl_2$ in the "dry" sample. The hygroscopicity of sinters had also been noticed with similar Fe(III) compounds [14].

The last, third decomposition step of $(Et_4N)_2[FeCl_4]$ in the inert atmosphere results in formation of a new phase of iron represented in the spectrum by sextet with parameters IS = 0.19(1) mm/s and H = 208.6(2) kOe (Fig. 6(c)) corresponding to cementite Fe_3C. It seems reasonable to conclude that in the third decomposition step some part of $FeCl_2$ is transformed into carbide. A small quantity (10%) of iron is present in a form of $[FeCl_4]^{2-}$ ions what suggest the incomplete decomposition of the sample.

A closer examination of the results obtained using Mössbauer spectroscopy and XRPD shows that $FeCl_2$ is the major product of the second decomposition step of $(Et_4N)_2[FeCl]_4$ (cf. the above equation), while the final products of the decomposition in the inert

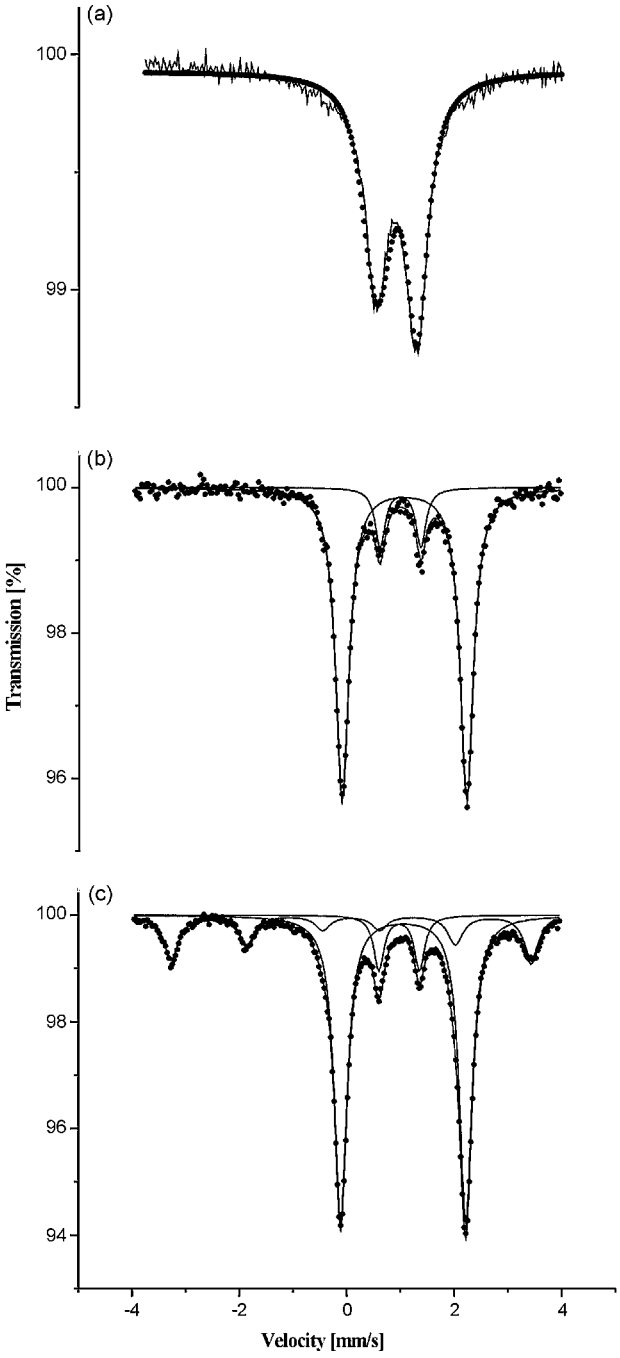

Fig. 6. Room temperature Mössbauer spectra of $(Et_4N)_2[FeCl_4]$ (a) and its products of the second, 833 K (b) and third, 1073 K (c) decomposition steps.

Table 2
Mössbauer parameters for $(Et_4N)_2[FeCl_4]$ and products of its decomposition after second (833 K) and third (1073 K) decomposition steps.

Sample	Temperature of decomposition (K)	IS (mm/s)	QS (mm/s)	Γ (mm/s)	A (%)	Species
$(Et_4N)_2[FeCl_4]$ non-burnt	–	0.92(06)	0.75(12)	0.24	100	$[FeCl_4]^{2-}$
Decomposition product	833	1.16(1)	2.32(1)	0.15(1)	87.5(5)	Fe^{2+}
		1.09(1)	0.76(1)	0.11(1)	12.5(4)	$[FeCl_4]^{2-}$
Decomposition product	1073	1.16(1)	2.32(1)	0.14(1)	67.5(2)	Fe^{2+}
		1.09(1)	0.76(1)	0.12(1)	9.7 ± 1.7	$[FeCl_4]^{2-}$
		0.19(1)		0.17(1)	22.8(7)	Fe_3C

atmosphere are $FeCl_2$ and Fe_3C. It was, however, interesting to learn in what form chlorine was released during conversion of $FeCl_2$ to Fe_3C, because in the MS spectra no unambiguous ionic currents due either to HCl or Cl_2 have been noticed.

Furthermore, it is also interesting to note that $FeCl_2$ predominates in the decomposition products of $(Et_4N)[FeCl_4]$ [17] at 683 K and that both phases, $FeCl_2$ and Fe_3C, occur in the final decomposition products of $(Et_4N)[FeCl_4]$. Thus both complexes $(Et_4N)[FeCl_4]$ and $(Et_4N)_2[FeCl_4]$ afford identical products during thermal transformations. The only difference consists in the quantities of $FeCl_2$ and Fe_3C which are smaller in the case of $(Et_4N)[FeCl_4]$ decomposition. In the spectrum of its final decomposition products in the argon atmosphere dominates a doublet with parameters IS = 1.09 mm/s and QS = 0.78 mm/s assignable to $[FeCl_4]^{2-}$. This may be explained in terms of a preliminary reduction of Fe(III) to Fe(II) to afford a labile phase (in the spectrum doublet with parameters IS = 1.15(1) mm/s and QS = 1.65(1) mm/s) attributed to $[FeCl_5]^{3-}$ [17,24] followed by the formation of $[FeCl_4]^{2-}$ at a higher temperature, whereas in $(Et_4N)_2[FeCl_4]$ the $[FeCl_4]^{2-}$ phase occurs just at the starting point.

Additionally, from a comparison of the results with those previously reported for analogous compounds of Fe(III), Co(II) and Cu(II) [17,20,21] some conclusions can be drawn on the influence of the oxidation state and the nature of the metal in the complexes on their thermal behaviour. For instance, with $(Et_4N)_2[FeCl_4]$ and $(Et_4N)[FeCl_4]$, the final decomposition products are identical ($FeCl_2$ and Fe_3C). It suggests that the oxidation state of the metal in a complex compound does not significantly affect its thermal decomposition pattern, the major decomposition products are virtually identical. However, some differences between the compounds remain still noticeable. On the other hand, a comparison of $(Et_4N)[FeCl_4]$ [17], $(Et_4N)_2[CoCl_4]$ [20] and $(Et_4N)_2[CuCl_4]$ [21] reveals some distinct differences. For instance, the final decomposition products of $(Et_4N)_2[CoCl_4]$ in an inert atmosphere are $CoCl_2$ and Co_2C (similar to Fe), whereas $(Et_4N)_2[CuCl_4]$ leaves behind elemental copper as the main product.

4. Conclusions

Bis(tetraethylammonium) tetrachloroferrate(II) undergoes thermal decomposition in three successive steps in the inert atmosphere. During the first two steps, ethyl chloride and triethylamine are released to leave behind $FeCl_2$. Upon further heating, Fe_3C is formed. Bearing all this in mind, the most probable decomposition course of $(Et_4N)_2[FeCl_4]$ can be described by the following equation:

$$(Et_4N)_2[FeCl_4] \xrightarrow[-EtCl_{(g)},\, Et_3N_{(g)}]{533-588\,K} ? \xrightarrow[-EtCl_{(g)},Et_3N_{(g)}]{588-678\,K} FeCl_2$$

$$+C_xH_yN_z \xrightarrow{678-1023\,K} FeCl_2 + Fe_3C$$

where $C_xH_yN_z$ denotes undecomposed organic residue

Because the first step is very vigorous and followed immediately by the second one, products of both steps are likely to occur in a sinter left behind at 588 K, this making difficult the analysis of the resulting solid and unambiguous the determination of its composition.

To sum up, the oxidation state of the metal in a complex compound does not significantly affect its thermal decomposition pattern. The final decomposition products of $(Et_4N)_n[FeCl_4]$ (n = 1 and 2) are $FeCl_2$ and Fe_3C. However, the kind of the metal in the complex anion has an influence on the pathway of thermal degradation of $(Et_4N)_2[MCl_4]$, where M is a metal(II). The final decomposition product of $(Et_4N)_2[CuCl_4]$ is elemental copper, whereas $(Et_4N)_2[CoCl_4]$ and $(Et_4N)_2[FeCl_4]$ leave behind a mixture consisting of metal(II) chloride and metal carbide.

More comparative evidence with other metal(II) ions will be provided after termination of the on-going research.

Acknowledgements

This research was supported by the Polish State Committee for Scientific Research under grant DS/8232-4-0088-8 and BW/8000-5-0454-8.

References

[1] J.W. Lauher, J.A. Ibers, Inorg. Chem. 14 (1975) 348–352.
[2] I.G. Gusakovskaya, S.I. Pirumowa, N.S. Ovanesyan, N.I. Golovina, R.F. Trofimova, G.V. Shilov, E.A. Lavrent'eva, Zh. Obshch. Khim. 68 (1998) 1264–1269.
[3] N.S. Gill, J. Chem. Soc. (1961) 3512–3515.
[4] A. Sabatini, L. Sacconi, J. Am. Chem. Soc. 86 (1964) 17–20.
[5] J.S. Afery, C.D. Burbridge, D.M.L. Goodgame, Spectochim. Acta 24A (1968) 1721–1726.
[6] R.J.H. Clark, T.M. Dunn, J. Chem. Soc. (1963) 1198–1201.
[7] D.M. Adams, J. Chatt, J.M. Davidson, J. Gerratt, J. Chem. Soc. (1963) 2189–2194.
[8] C.D. Burbridge, D.M. Goodgame, J. Chem. Soc. A (1968) 1074–1079.
[9] H. Kobayashi, H. Cui, A. Kobayashi, Chem. Rev. 104 (2004) 5265–5288.
[10] T. Enoki, A. Miyazaki, Chem. Rev. 104 (2004) 5449–5477.
[11] T. Wyrzykowski, A. Maniecki, J. Pattek-Janczyk, Z. Stanek, Warnke, Thermochim. Acta 435 (2005) 92–98.
[12] D. Wyrzykowski, R. Kruszyński, U. Kucharska, Z. Warnke, Z. Anorg. Allg. Chem. 632 (2006) 624–628.
[13] D. Wyrzykowski, R. Kruszyński, Acta Crystallogr. E62 (2006) m994–m996.
[14] D. Wyrzykowski, R. Kruszyński, T. Maniecki, Z. Warnke, Z. Anorg. Allg. Chem. 633 (2007) 285–289.
[15] D. Wyrzykowski, R. Kryszyński, J. Kłak, J. Mroziński, Z. Warnke, Z. Anorg. Allg. Chem. 633 (2007) 2071–2076.
[16] D. Wyrzykowski, T. Maniecki, M. Gazda, E. Styczeń, Z. Warnke, J. Therm. Anal. Cal. 90 (2007) 893–897.
[17] D. Wyrzykowski, A. Pattek–Janczyk, T. Maniecki, K. Zaremba, Z. Warnke, J. Therm. Anal. Cal. 91 (2008) 279–284.
[18] ICDD PDF-2 Database Release 1998, ISNN 1084-3116.
[19] A. Bujewski, K. Grzedzicki, J. Błażejowski, Z. Warnke, J. Therm. Anal. Cal. 33 (1988) 961.
[20] E. Styczeń, Z. Warnke, D. Wyrzykowski, Thermochim. Acta 454 (2007) 84–89.
[21] E. Styczeń, W.K. Jóźwiak, M. Gazda, D. Wyrzykowski, Z. Warnke, J. Therm. Anal. Cal. 91 (2008) 979–984.
[22] P.R. Edwards, C.E. Johnson, R.J.P. Williams, J. Chem. Phys. 47 (1967) 2074–2082.
[23] N.N. Greenwood, T.C. Gibb, Mössbauer Spectroscopy, Chapman and Hall, London, 1972.
[24] M. Feist, S.I. Troyanov, H. Mehner, K. Witke, E. Kemnitz, Z. Anorg. Allg. Chem. 625 (1999) 141–146.